

# Robust $H_2$ Synthesis for Dual-stage Multi-sensing Track-following Servo Systems in HDDs

Ryozo Nagamune, Xinghui Huang, and Roberto Horowitz

**Abstract**—This paper presents a robust  $H_2$  synthesis technique for designing a track-following servo system for a hard disk drive (HDD) product line. The goal is to design a single robust controller that minimizes the worst case  $H_2$  performance of an entire disk drive product line, assuming that dynamic variations in the product line (i.e. variations from one unit to another) are accurately characterized by affine variations in several of the actuator’s model parameters, such as variations in the resonance frequency or damping ratio of a resonance mode. The advantages and disadvantages of the proposed method are discussed and an illustrative realistic example is presented.

## I. INTRODUCTION

Track-following control of the magnetic read/write head in hard disk drives (HDDs) is of great importance in meeting recent and future requirements of extremely high track density. For a given system consisting of several components such as a suspension, sensors, and actuators, the track-following servo system control should attain the smallest possible track-misregistration, which is generally measured by the variance of the position error signal (PES), in the presence of measurement noise, track runout, windage, and external shock. In addition to optimality, *robustness* is essential in track-following control. In addition to the many disturbances that affect the control system, a controller has to be designed so that it maintains an acceptable track-following performance when installed in hundreds of thousands of HDD units of a given product line, where each unit may have slightly different dynamics. This paper proposes a robust and optimal control design methodology for a general servo system, which will be referred to as a *dual-stage multi-sensing (DSMS)* system. The DSMS system has two actuators and several sensor measurements, and is expected to be necessary for achieving highly precise track-following in future HDDs. For this multivariable control system, it is not easy to systematically design a controller that provides both optimality and robustness by using classical control theory. Therefore, we will apply a recently developed robust  $H_2$  synthesis theory [6] to the proposed DSMS system.

In order to enhance performance, it is advantageous to exploit the freedom of using different sampling/hold rates in the DSMS system. In HDDs, the attainable sampling rate of the PES is generally limited by the disk spinning speed and the number of servo sectors in the disk, while

the sampling/hold rates of other sensors, such as a sensor measuring the head relative to the suspension tip, or a vibration sensor in the suspension, are not subjected to these limitations. It is natural to presume that an increase of these sample rates will improve track-following performance. In this paper, we will assume arbitrary sampling/hold rates.

The paper is organized as follows. In Section II, a multirate robust track-following problem is formulated mathematically. To solve the formulated problem, Section III presents a robust  $H_2$  synthesis method developed in [6]. Section IV gives a simple example for dual-stage control with the robust  $H_2$  synthesis technique. The linear matrix inequalities (LMIs) used in this paper are presented in the Appendix.

## II. A ROBUST TRACK-FOLLOWING CONTROL PROBLEM

In this section, we will formulate a multirate robust track-following control problem to be tackled in this paper. The formulation is general enough to cover most of the track-following control problems encountered in the magnetic disk drive industry, such as single-stage and dual-stage control, irrespective of the type of the secondary actuator, and the locations/number of sensors. Practical examples of track-following control which reduce to the formulation given below will be presented in Section IV, as well as in [3].

Let us consider a discrete-time<sup>1</sup> linear time-invariant generalized plant with an uncertainty block (see Fig. 1):

$$\begin{bmatrix} z_\Delta \\ z_2 \\ y \end{bmatrix} = \begin{bmatrix} A & B_\Delta & B_2 & B_u \\ C_\Delta & D_{\Delta\Delta} & D_{\Delta 2} & D_{\Delta u} \\ C_2 & D_{2\Delta} & D_{22} & D_{2u} \\ C_y & D_{y\Delta} & D_{y2} & 0 \end{bmatrix} \begin{bmatrix} w_\Delta \\ w_2 \\ u \end{bmatrix}, \quad (1)$$

$$w_\Delta = \Delta z_\Delta, \quad (2)$$

where we have used the standard notation:

$$\left[ \begin{array}{c|c} A & B \\ \hline C & D \end{array} \right] := D + C(zI - A)^{-1}B. \quad (3)$$

Here,  $u$  is the input vector of length 2, which consists of signals to the voice coil motor (VCM) and an auxiliary mini- or micro-actuator.  $y$  is the measurement vector (of any length), typically consisting of the PES, the suspension vibration signal measured by PZT sensors, the position of the magnetic head relative to the gimbal, as measured by a microactuator relative position sensor, and so on.  $z_2$  is the control output vector, typically consisting of the PES and input amplitudes, and  $w_2$  is the disturbance vector of

This work was supported by the Information Storage Industry Consortium (INSIC), the Computer Mechanics Laboratory (CML) at UC Berkeley and the Swedish Research Council (VR).

The authors are with the Department of Mechanical Engineering, University of California, Berkeley, CA 94720, USA. {ryozo, xhhuang, horowitz}@me.berkeley.edu.

<sup>1</sup>Throughout this paper, we assume that, if a plant model is originally given in continuous-time, it has been discretized with the fastest sampling/hold rate.

all undesirable signals, such as track runout, windage, and measurement noise. All the matrices in (1) are constant and assumed to have compatible dimensions. The generalized plant is comprised of the VCM and secondary actuator dynamics, as well as weighting functions.

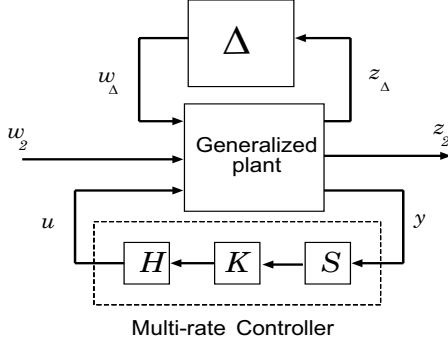


Fig. 1. A generalized plant with an uncertainty block  $\Delta$  and a multirate controller  $HKS$

The uncertainty block  $\Delta$  is assumed to be a diagonal matrix in the set:

$$\mathcal{B} := \{ \Delta := \text{diag} [\delta_1, \dots, \delta_p], \delta_j \in B\mathbb{R}, j = 1, \dots, p \}, \quad (4)$$

where  $p$  is the number of parametric uncertainties, and  $B\mathbb{R} := \{r \in \mathbb{R} : |r| \leq 1\}$ . The real uncertainty  $\delta_j$  is interpreted as a parameter variation in the dynamics of the VCM and the auxiliary actuator, such as gain, damping ratio and resonance frequency.

**Remark 1:** It may happen that some parametric uncertainties appear repeatedly as  $\delta_j I$ . However, since the subsequent discussions are almost unchanged even in such cases, we just consider the case of non-repeated parametric uncertainties.

Denote the operator from  $w_2$  to  $z_2$  by  $T_{z_2 w_2}$ . This operator depends on the uncertainty  $\Delta$  and a multirate controller  $HKS$ , where  $S$  and  $H$  mean a multirate sampler and a multirate hold, respectively. Thus, we show the dependence explicitly as  $T_{z_2 w_2}(HKS, \Delta)$ . Note that the operator  $T_{z_2 w_2}(HKS, \Delta)$  is time-varying in general due to the multirate sampler and hold. Then, a multirate robust track-following control problem can be formulated as follows.

**Problem 1:** For given multirate sampler  $S$  and hold  $H$  with fixed sampling and hold rates, design a controller  $K$  that stabilizes exponentially the closed-loop system for all  $\Delta \in \mathcal{B}$ , and minimizes the worst-case RMS value of  $z_2$  against Gaussian white noise  $w_2$ , or equivalently, solve the optimization problem

$$\min_{K \in \mathcal{K}(\mathcal{B})} \max_{\Delta \in \mathcal{B}} \|T_{z_2 w_2}(HKS, \Delta)\|_2, \quad (5)$$

where  $\mathcal{K}(\mathcal{B})$  is the set of all controllers that exponentially stabilize the closed-loop system for all  $\Delta \in \mathcal{B}$ , and  $\|\cdot\|_2$  denotes the  $\ell_2$  semi-norm defined for time-varying systems in [13, p. 73].

This is a multirate robust performance synthesis problem with parametric uncertainties. We remark that this problem is general in that it contains, as special cases, single-stage single-sensing cases, as well as single-rate cases.

### III. ROBUST CONTROLLER DESIGN

In this section, we will review the robust  $H_2$  synthesis technique in [6], which is useful for robust track-following. The method is based on convex optimization involving LMIs, to which there are numerically efficient algorithms [11] and software [16], [2], [8] available. Some of the LMIs which are necessary to solve optimization problems proposed in this paper will be given in the Appendix. Advantages and disadvantages of the method will be summarized.

To use the result in [6], we need to assume that  $D_{\Delta\Delta} = 0$  and  $D_{y\Delta} = 0$  in (1). The assumption  $D_{\Delta\Delta} = 0$  guarantees that the closed-loop system matrices depend on  $\Delta$  affinely (see (7)), while  $D_{y\Delta} = 0$  ensures the well-posedness of the closed-loop system by forcing the direct term from  $u$  to  $y$  to be zero (see (6)). These assumptions are not restrictive, since they hold most of the track-following problems in HDDs.

In the case with only parametric uncertainties, the uncertain system from  $[w_2^T, u^T]^T$  to  $[z_2^T, y^T]^T$  is obtained as

$$\begin{bmatrix} z_2 \\ y \end{bmatrix} = \begin{bmatrix} A^\Delta & B_2^\Delta & B_u^\Delta \\ C_2^\Delta & D_{22}^\Delta & D_{2u}^\Delta \\ C_y & D_{y2} & 0 \end{bmatrix} \begin{bmatrix} w_2 \\ u \end{bmatrix}, \quad (6)$$

where the superscript “ $\Delta$ ” means a “matrix with uncertainties”, and the system matrices are given by

$$\begin{bmatrix} A^\Delta & B_2^\Delta & B_u^\Delta \\ C_2^\Delta & D_{22}^\Delta & D_{2u}^\Delta \end{bmatrix} := \begin{bmatrix} A & B_2 & B_u \\ C_2 & D_{22} & D_{2u} \end{bmatrix} + \begin{bmatrix} B_\Delta \\ D_{2\Delta} \end{bmatrix} \Delta \begin{bmatrix} C_\Delta & D_{\Delta 2} & D_{\Delta u} \end{bmatrix}. \quad (7)$$

In the robust  $H_2$  method that will be explained below, it is important that the system matrices in (7) are affine in  $\Delta$ , and that  $\Delta$  belongs to a convex polyhedron  $\mathcal{B}_p$  (which is a hypercube in the present setting).

To deal with the multirate characteristics of the controller, we can use the procedure in [7], [10]. By combining the system (6) with multirate sampler and hold, we can obtain a periodic time-varying system of the form (see [10] for details):

$$\begin{bmatrix} \tilde{x}(k+1) \\ z_2(k) \\ \tilde{y}(k) \end{bmatrix} = \begin{bmatrix} \tilde{A}^\Delta(k) & \tilde{B}_2^\Delta(k) & \tilde{B}_u^\Delta(k) \\ \tilde{C}_2^\Delta(k) & \tilde{D}_{22}^\Delta(k) & \tilde{D}_{2u}^\Delta(k) \\ C_y(k) & \tilde{D}_{y2}(k) & 0 \end{bmatrix} \begin{bmatrix} \tilde{x}(k) \\ w_2(k) \\ \tilde{u}(k) \end{bmatrix}, \quad (8)$$

for  $k = 0, 1, 2, \dots, N-1$ , with a certain period  $N$ . (Here,  $\tilde{y} = Sy$  and  $u = H\tilde{u}$ .) Then, for an auxiliary time-invariant plant constructed with the matrices in (8):

$$\begin{bmatrix} z_2 \\ y \end{bmatrix} = \begin{bmatrix} ZA^\Delta & ZB_2^\Delta & ZB_u^\Delta \\ C_2^\Delta & D_{22}^\Delta & D_{2u}^\Delta \\ C_y & D_{y2} & 0 \end{bmatrix} \begin{bmatrix} w_2 \\ u \end{bmatrix}, \quad (9)$$

where  $A^\Delta := \text{blockdiag} [\tilde{A}^\Delta(0), \dots, \tilde{A}^\Delta(N-1)]$  ( $B_2^\Delta$  etc. are defined similarly), and  $Z$  is a shift matrix, we need

to design a linear time-invariant controller of the form:

$$\mathbf{u} = \begin{bmatrix} \mathbf{Z}\mathbf{K}_A & \mathbf{Z}\mathbf{K}_B \\ \mathbf{K}_C & \mathbf{K}_D \end{bmatrix} \mathbf{y}. \quad (10)$$

By decomposing the block-diagonal matrices  $\mathbf{K}_A$  etc. in (10), we can recover a periodic time-varying controller for our original problem as

$$\begin{cases} x_K(k+1) &= K_A(k)x_K(k) + K_B(k)\tilde{y}(k), \\ \tilde{u}(k) &= K_C(k)x_K(k) + K_D(k)\tilde{y}(k). \end{cases} \quad (11)$$

for  $k = 0, \dots, N-1$ .

We remark that all the uncertain matrices in (9) are affine in  $\Delta$ . The time-invariant closed-loop system of (9) and (10) is expressed as

$$\begin{aligned} (T_{cl}(\Theta, \Delta))(z) &:= \begin{bmatrix} A_{cl}(\Theta, \Delta) & B_{cl}(\Theta, \Delta) \\ C_{cl}(\Theta, \Delta) & D_{cl}(\Theta, \Delta) \end{bmatrix}, \\ &:= \begin{bmatrix} \mathbf{Z}(A_0^\Delta + \mathfrak{B}^\Delta \Theta \mathfrak{C}) & \mathbf{Z}(B_0^\Delta + \mathfrak{B}^\Delta \Theta \mathfrak{D}_{21}) \\ C_0^\Delta + \mathfrak{D}_{12}^\Delta \Theta \mathfrak{C} & D_{22}^\Delta + \mathfrak{D}_{12}^\Delta \Theta \mathfrak{D}_{21} \end{bmatrix}, \end{aligned}$$

where the matrices are defined by

$$\begin{aligned} \mathbf{Z} &:= \begin{bmatrix} Z & 0 \\ 0 & Z \end{bmatrix}, \quad \Theta := \begin{bmatrix} \mathbf{K}_A & \mathbf{K}_B \\ \mathbf{K}_C & \mathbf{K}_D \end{bmatrix}, \\ A_0^\Delta &:= \begin{bmatrix} \mathbf{A}^\Delta & 0 \\ 0 & 0 \end{bmatrix}, \\ \mathfrak{B}^\Delta &:= \begin{bmatrix} 0 & B_u^\Delta \\ I & 0 \end{bmatrix}, \quad B_0^\Delta := \begin{bmatrix} B_{y2}^\Delta \\ 0 \end{bmatrix}, \\ \mathfrak{C} &:= \begin{bmatrix} 0 & I \\ C_y & 0 \end{bmatrix}, \quad \mathfrak{D}_{21} := \begin{bmatrix} 0 \\ D_{y2} \end{bmatrix}, \\ C_0^\Delta &:= \begin{bmatrix} C_2^\Delta & 0 \end{bmatrix}, \quad \mathfrak{D}_{12}^\Delta := \begin{bmatrix} 0 & D_{2u}^\Delta \end{bmatrix}. \end{aligned}$$

Our problem is to find a robustly stabilizing controller matrix  $\Theta$  that solves

$$\min_{\Theta} \max_{\Delta \in \mathcal{B}_p} \|T_{cl}(\Theta, \Delta)\|_2.$$

This can be solved by the following optimization, which involves a finite number of matrix inequalities:

$$\begin{aligned} &\min_{\mathbf{W}, \mathbf{P}, \Theta} \gamma, \text{ subject to} \\ &\left\{ \begin{array}{l} \gamma > \text{trace} \mathbf{W} \\ \begin{bmatrix} \mathbf{W} & C_{cl}(\Theta, \Delta_k) & D_{cl}(\Theta, \Delta_k) \\ * & \mathbf{P} & 0 \\ * & * & I \end{bmatrix} > 0, \\ \begin{bmatrix} \mathbf{P}_Z & \mathbf{P}_Z A_{cl}(\Theta, \Delta_k) & \mathbf{P}_Z B_{cl}(\Theta, \Delta_k) \\ * & \mathbf{P} & 0 \\ * & * & I \end{bmatrix} > 0, \end{array} \right. \end{aligned} \quad (12)$$

for  $\Delta_k \in \mathcal{V}(\mathcal{B}_p)$ . Here, the matrices  $\mathbf{P}$  and  $\mathbf{W}$  are block-diagonal of appropriate sizes,  $\mathbf{P}_Z := \mathbf{Z}^T \mathbf{P} \mathbf{Z}$ ,  $\mathcal{V}(\mathcal{B}_p)$  is the set of all vertices of a convex polyhedron  $\mathcal{B}_p$ , and the “\*-blocks” are the block matrices that make the total matrix symmetric. The replacement of infinitely many inequality constraints for  $\Delta \in \mathcal{B}_p$  with finitely many ones at vertices  $\Delta_k \in \mathcal{B}_p$  is possible due to the facts that the closed-loop system matrices are affine in  $\Delta$ , and that the set  $\mathcal{B}_p$  is a convex polyhedron.

Unfortunately, this problem is nonconvex, since there are coupling terms between  $\mathbf{P}$  and  $\Theta$  in (12). However, by using the coordinate descent method (see [5], [4] and references therein), we can find a local optimum. The procedure is presented next.

**[Initial design of  $\Theta$ ]** This will be explained below, as well as in Appendix I. Set the result of the initial design to  $\Theta_0$ . Also, set  $i = 1$ .

**[Design of  $\mathbf{P}$ ]** Fix  $\Theta := \Theta_i$ . Solve a convex optimization problem (12) with respect to  $\gamma$ ,  $\mathbf{W}$ , and  $\mathbf{P}$ . Set a solution  $\mathbf{P}$  to  $\mathbf{P}_i$ .

**[Design of  $\Theta$ ]** Fix  $\mathbf{P} := \mathbf{P}_i$ . Solve a convex optimization problem (12) with respect to  $\gamma$ ,  $\mathbf{W}$ , and  $\Theta$ . Set a solution  $\Theta$  to  $\Theta_{i+1}$ . Increment  $i$  by one. Continue this iteration until convergence.

Generally speaking, in nonconvex optimization problems, the selection of an initial point is critical. We follow the procedure given in [6] to derive a reasonable initial point, which will be reviewed in Appendix I.

The advantage of the robust  $H_2$  synthesis is the ability to cope with robust performance in the design. However, to utilize the proposed synthesis technique, it is necessary to ignore dynamic uncertainties. In addition, the computation of a solution to the robust  $H_2$  problem is demanding, because we have to solve a series of convex optimization problems iteratively in order to solve a nonconvex problem. Further, the number of inequality constraints increases exponentially with the number of parametric uncertainties, since the constraints are imposed at vertices of a hypercube  $\mathcal{B}_p$ . Therefore, only a few parametric uncertainties can be included in a practical design.

#### IV. A DESIGN EXAMPLE

In this section, we will demonstrate the usefulness of the robust  $H_2$  synthesis method presented in Section III through one simple example of a dual-stage track-following control problem. This example is taken from [1]. Other examples will be shown in [3]. The system to be considered is a PZT-actuated dual-stage servo system, whose inputs are the VCM input ( $u_V$ ) and the input to PZT-microactuator ( $u_M$ ), and whose output is the head position ( $y_{LDV}$ ) measured by LDV. The transfer functions from the inputs  $u_V$  and  $u_M$  to the output  $y_{LDV}$  are respectively denoted  $P_{VCM}$  and  $P_{MA}$ .

##### A. Continuous-time modeling

In order to use the robust  $H_2$  synthesis technique, we need a mathematical model that has only parametric uncertainties, and accurately describes unit-to-unit variations in a HDD product line. Such a mathematical model can be derived from frequency responses. 36 frequency experimentally obtained responses of  $P_{VCM}$  and  $P_{MA}$  were obtained in [1], as shown in Figure. 2.

To reduce control synthesis computational burden, it is advantageous to build a model in which both the order and number of uncertain parameters is as small as possible. In

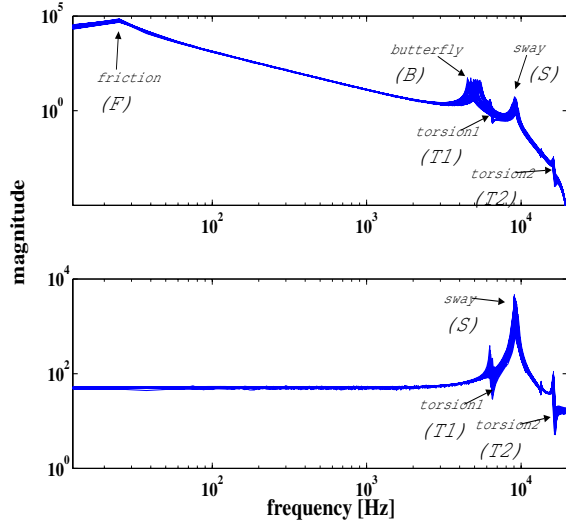


Fig. 2. Frequency responses from  $u_V$  to  $y_{LDV}$  (upper figure) and from  $u_M$  to  $y_{LDV}$  (lower figure)

Figure 2, since the sway mode (S) and the torsion modes (T1 and T2) can be seen in both frequency responses, these suspension modes  $P_{ma}$  can be factored out as shown in the block diagram in Figure 3:

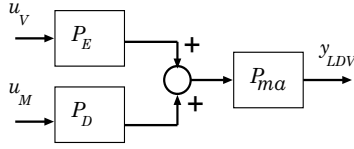


Fig. 3. Block diagram

$$P_{VCM}(s) = P_{ma}(s)P_E(s), \quad P_{MA}(s) = P_{ma}(s)P_D(s). \quad (13)$$

Here, the E-block dynamics  $P_E$  and suspension dynamics  $P_{ma}$  are assumed to have structures as

$$P_E(s) = P_F(s)P_B(s), \quad (14)$$

$$P_{ma}(s) = P_{T1}(s)P_S(s)P_{T2}(s), \quad (15)$$

where each term of the right-hand sides is of the form

$$P_j(s) = \frac{b_0^j s^2 + b_1^j s + b_2^j}{s^2 + a_1^j s + a_2^j}, \quad j = F, B, T1, S, T2, \quad (16)$$

with uncertain coefficients

$$b_k^j = \bar{b}_k^j (1 + M_{bk}^j \delta^j), \quad k = 1, 2, \quad (17)$$

$$a_k^j = \bar{a}_k^j (1 + M_{ak}^j \delta^j), \quad k = 1, 2. \quad (18)$$

Here, the nominal values are denoted by  $\bar{a}_k^j$  and  $\bar{b}_k^j$ , and  $M_{ak}^j$  and  $M_{bk}^j$  are constant weightings. It has been found that the experimental frequency responses can be reproduced accurately enough by using only three uncertain parameters

$$\delta_1 = \delta^F, \quad \delta_2 = \delta^B, \quad \delta_3 = \delta^{T1} = \delta^{T2} = \delta^S. \quad (19)$$

$P_D$  is the piezoelectric actuator driver dynamics that is not observed in  $P_{VCM}$ , and of the form

$$P_D(s) = b_1^D s + b_2^D. \quad (20)$$

Assuming the structure of the model (13)–(20), the nominal values and the weighting coefficients are identified as in Table I. The validity of the modeling result will be examined

mode $j$	$\bar{b}_0^j$	$\bar{b}_1^j$	$\bar{b}_2^j$	$\bar{a}_1^j$	$\bar{a}_2^j$
$F$	0	0	4.206e8	51.175	2.365e4
$B$	0	0	1.003e9	569.8	1.003e9
$T1$	1	720	1.598e9	208.2	1.575e9
$S$	0	0	3.316e9	1015	3.316e9
$T2$	1	6300	1.079e10	2700	1.02e10
$D$	–	4.0026e-4	47.3151	–	–

mode $j$	$M_{b1}^j$	$M_{b2}^j$	$M_{a1}^j$	$M_{a2}^j$
$F$	0	0.3	0	0
$B$	0	0.35	0	0.35
$T1$	-0.03	-0.03	0	0.05
$S$	0	0.12	0.1	0.12
$T2$	-0.01	-0.01	0	0.05

TABLE I

NOMINAL PARAMETERS AND WEIGHTING COEFFICIENTS VALUES

after the discretization of the model set in Section IV-B.

#### B. Discretization of a continuous-time model set

For digital controller design, the continuous-time uncertain model is transformed into a discrete-time one. Although there are several ways to carry out such transformation, we present only one method here.

The block diagram in Figure 3 can be expressed as an LFT form with uncertain parameters as in Figure 4. We can

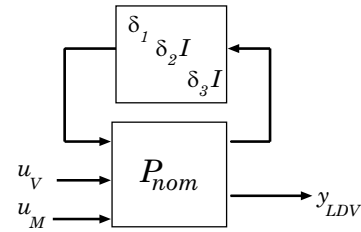


Fig. 4. Block diagram with parametric uncertainties:  $P_{nom}$  is a nominal plant

represent the continuous-time model set from  $[u_V, u_M]^T$  to  $y_{LDV}$  as

$$\mathcal{P}_c = \left\{ \begin{array}{l} P(s) = D + C(sI - A(\Delta))^{-1}B(\Delta) \\ \Delta = \text{diag}[\delta_1, \delta_2 I, \delta_3 I], \quad |\delta_i| \leq 1, \forall i \end{array} \right\}. \quad (21)$$

Since there are three uncertain parameters  $\delta_i$ , the set  $\mathcal{P}_c$  has  $2^3$  “extreme” cases denoted by  $\Delta_i$ , where each parameter  $\delta_i$  takes the value of  $-1$  or  $1$ . For each extreme case, we transform the continuous-time model into a discrete-one by zero-order hold, yielding discrete-time  $(A, B)$ -matrices as follows:

$$A_d^i := e^{A(\Delta_i)T}, \quad B_d^i := \int_0^T e^{A(\Delta_i)\tau} d\tau \cdot B(\Delta_i),$$

where  $T = 25 \cdot 10^{-6}$  (sec.) is a sampling period. For controller design, we use all the convex combinations of these eight discrete-time  $(A, B)$ -matrices:

$$\mathcal{P}_d := \{P(z) = D + C(zI - A)^{-1}B, [A, B] \in \mathcal{B}\},$$

where

$$\mathcal{B} := \left\{ [A, B] = \sum_{i=1}^8 \alpha_i [A_d^i, B_d^i], \alpha_i \geq 0, \sum_{i=1}^8 \alpha_i = 1 \right\}.$$

The comparisons between experimental frequency responses and those of sampled models in the model set  $\mathcal{P}_d$  have been shown in Figures 5 and 6. Both figures show that the observed dynamic variation can be accurately represented by the parametric uncertainty modeling technique.

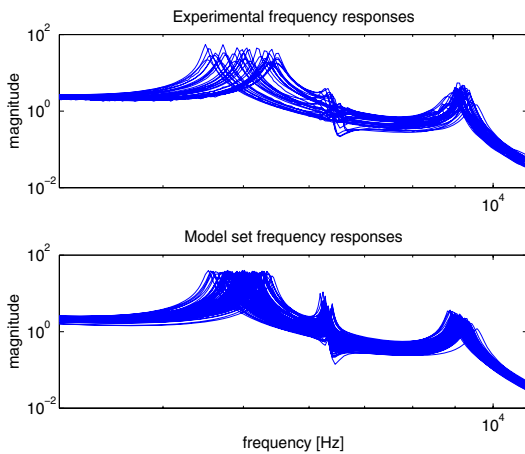


Fig. 5. Comparisons between experimental and simulation frequency responses for  $P_{VCM}$

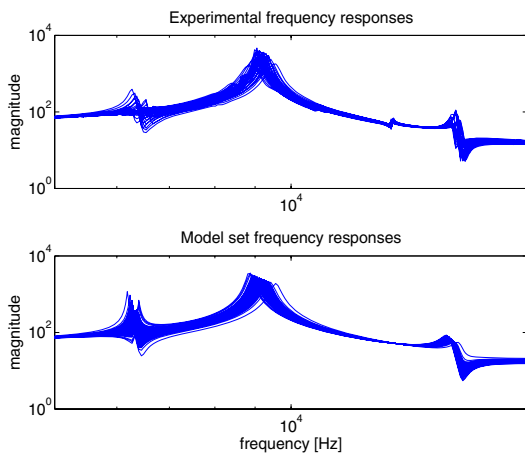


Fig. 6. Comparisons between experimental and simulation frequency responses for  $P_{MA}$

### C. Controller design via robust $H_2$ synthesis

To determine a controller design problem, we need to specify the variables  $z_2$ ,  $w_2$ ,  $y$  and  $u$  in (6). In this example,

control inputs  $u$  are taken as

$$u := [u_V, u_M]^T.$$

As a disturbance, in this simple example, we consider only track runout  $r$ , modeled as

$$r = W_r w_2,$$

where  $W_r$  is a shaping filter

$$W_r(s) = \frac{3.162s + 1.987 \cdot 10^5}{s + 628.3},$$

and  $w_2$  is white noise (This  $w_2$  corresponds to the one in (6)). The difference between  $r$  and  $y_{LDV}$

$$e := r - y_{LDV}$$

is the PES, which is the measurement  $y$  in (6). As control outputs  $z$ , we use the vector consisting of the PES and weighted input signals as

$$z := [e, Q_V u_V, Q_M u_M]^T,$$

where the weights  $Q_V$  and  $Q_M$  are selected by trial-and-error as  $Q_V = 0.1$  and  $Q_M = 5 \cdot 10^{-5}$ .

The designed controller was of order 13. In order to analyze the controller, the sensitivity functions for 100 sampled models are shown in Figure 7. As can be seen in the figure, the sensitivity functions do not disperse even in the face of parameter variations, indicating that the obtained controller indeed satisfies its intended robust performance property. This property was also verified during the experimental tests, as discussed in [1].

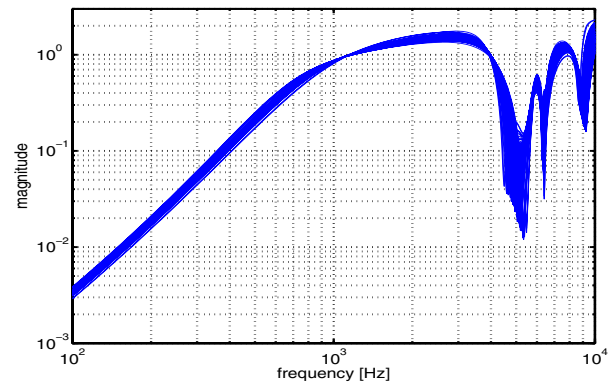


Fig. 7. Sensitivity functions

## V. CONCLUSIONS

In this paper, we have presented a multirate robust  $H_2$  controller design method for track-following control in dual-stage multi-sensing servo systems. The method relies on numerically efficient solvers for LMIs. One track-following control example for a PZT actuated suspension dual-stage system was given to illustrate that the robust  $H_2$  controller is useful in maintaining the track-following performance under plant perturbations. Other robust control techniques, such as mixed  $H_2/H_\infty$  and mixed  $H_2/\mu$  synthesis techniques [15],

[9], [12], are also useful for the track-following control. It is known that one major drawback of robust control theory is that the designed controllers typically have high orders. Therefore, controller reduction should also be done after all of the robust controller design procedures. Since a multirate controller is periodic time-varying in general, we can utilize the existing balanced truncation techniques, e.g., those in [17], [14], for the reduction purpose. Some additional realistic examples in [3] show that the proposed design methodologies, combined with model reduction techniques, are quite promising in designing low order controllers with robust track-following performance.

#### ACKNOWLEDGMENT

The authors are grateful to Professor Raymond de Callafon at the University of California, San Diego, for providing them with the experimental data in the dual-stage servo example.

#### REFERENCES

- [1] R. A. de Callafon, R. Nagamune, and R. Horowitz. Robust dynamic modeling and control of dual-stage actuators. Submitted for publication to the IEEE Transactions on Magnetics.
- [2] P. Gahinet, A. Nemirovski, A. J. Laub, and M. Chilali. *LMI Control Toolbox User's Guide*. Mathwork, 1995.
- [3] X. Huang, R. Nagamune, and R. Horowitz. A comparison of multirate robust track-following control synthesis techniques for dual-stage and multi-sensing servo systems in hard disk drives. Submitted for presentation to the 2006 American Control Conference.
- [4] T. Iwasaki. The dual iteration for fixed-order control. *IEEE Trans. Automat. Control*, 44(4):783–788, April 1999.
- [5] T. Iwasaki and R. E. Skelton. The XY-centering algorithm for the dual LMI problem: A new approach to fixed order control design. *Int. J. Control*, 62(6):1257–1272, 1995.
- [6] S. Kanev, C. Scherer, M. Verhaegen, and B. De Schutter. Robust output-feedback controller design via local bmi optimization. *Automatica*, 40, 2004.
- [7] S. Lall and G. Dullerud. An LMI solution to the robust synthesis problem for multi-rate sampled-data systems. *Automatica*, 37(12):1909–1922, 2001.
- [8] J. Löfberg. YALMIP : A toolbox for modeling and optimization in MATLAB. In *Proceedings of the CACSD Conference*, Taipei, Taiwan, 2004. Available from <http://control.ee.ethz.ch/~jloef/yalmip.php>.
- [9] I. Masubuchi, A. Ohara, and N. Suda. LMI-based controller synthesis: A unified formulation and solution. *Int. J. Robust and Nonlinear Control*, 8(8):669–686, 1998.
- [10] R. Nagamune, X. Huang, and R. Horowitz. Multi-rate track-following control with robust stability for a dual-stage multi-sensing system in HDDs. Technical report, Computer Mechanics Laboratory, University of California, Berkeley, 2005. Also to appear in the proceedings at the 44th IEEE Conference on Decision and Control.
- [11] Y. Nesterov and A. Nemirovskii. *Interior-Point polynomial algorithms in convex programming*. SIAM, 1994.
- [12] A. Packard and J. C. Doyle. The complex structured singular value. *Automatica*, 29(1):71–109, 1993.
- [13] M. A. Peters and P. A. Iglesias. *Minimum entropy control for time-varying systems*. Systems & Control: Foundations & Applications. Birkhäuser, 1997.
- [14] H. Sandberg and A. Rantzer. Balanced truncation of linear time-varying systems. *IEEE Trans. Automat. Control*, 49(2):217–229, February 2004.
- [15] C. Scherer, P. Gahinet, and M. Chilali. Multiobjective Output-Feedback Control via LMI Optimization. *IEEE Trans. Automat. Control*, 42(7):896–911, July 1997.
- [16] J. F. Sturm. Using SeDuMi 1.02, a matlab toolbox for optimization over symmetric cones. *Optimization Methods and Software*, 11–12:625–653, 1999. Special issue on Interior Point Methods.
- [17] A. Varga. Balanced truncation model reduction of periodic systems. In *Proceedings of the 39th IEEE Conference on Decision and Control*, pages 2379–2384, Sydney, Australia, December 2000.

#### APPENDIX I

##### INITIAL CONTROLLER DESIGN IN ROBUST $H_2$ SYNTHESIS

The robust  $H_2$  controller is designed via nonconvex optimization (12). For nonconvex optimization, selection of an initial point is of great importance. Here, we review a reasonable method for such selection proposed in [6].

##### A. State feedback

First, for the uncertain system (9), we design a state feedback controller  $u = K_C x$ , that optimizes robust  $H_2$  performance  $\max_{\Delta \in \mathcal{B}_p} \|T_{z_2 w_2}\|_2$ . As given in Theorem 6 in [6], this problem can be solved by convex optimization with LMIs:

$$\begin{aligned} & \min_{W, Q, L} \text{trace} W, \text{ subject to} \\ & \left\{ \begin{array}{l} \begin{bmatrix} W & C_2^\Delta Q + D_{2u}^\Delta L & D_{22}^\Delta \\ * & Q & 0 \\ * & * & I \end{bmatrix} > 0, \\ \begin{bmatrix} Q_Z & A^\Delta Q + B_u^\Delta L & B_2^\Delta \\ * & Q & 0 \\ * & * & I \end{bmatrix} > 0, \end{array} \right. \end{aligned} \quad (22)$$

where the constraints are imposed at the vertices of  $\mathcal{B}_p$ ,  $\Delta = \Delta_k \in \mathcal{V}(\mathcal{B}_p)$ . Using the solutions  $L$  and  $Q$ , the optimal state feedback is given by  $K_C := LQ^{-1}$ .

##### B. Output feedback

Next, by fixing  $K_C$  as above and  $K_D = 0$ , we design an output feedback

$$u = \begin{bmatrix} ZK_A & ZK_B \\ K_C & 0 \end{bmatrix} y. \quad (23)$$

that optimizes robust  $H_2$  performance. Define  $A_F^\Delta := A^\Delta + B_u^\Delta K_C$ . Then, due to Theorem 8 in [6], this problem can be solved by convex optimization with LMIs:

$$\begin{aligned} & \min_{W, X, Y, U, V} \text{trace} W, \text{ subject to} \\ & \left\{ \begin{array}{l} \begin{bmatrix} W & C_z^\Delta + D_{zu}^\Delta K_C & D_{zu}^\Delta K_C & D_{zw}^\Delta \\ * & X & 0 & 0 \\ * & * & Y & 0 \\ * & * & * & I \end{bmatrix} > 0, \\ \begin{bmatrix} X_Z & 0 & X_Z A_F^\Delta \\ * & Y_Z & Y_Z A_F^\Delta - V - UC_y \\ * & * & X \\ * & * & * \\ * & * & * \\ -X_Z B_u^\Delta K_C & X_Z B_w^\Delta \\ V - Y_Z B_u^\Delta K_C & Y_Z B_w^\Delta - UD_{yw} \\ 0 & 0 \\ Y & 0 \\ * & I \end{bmatrix} > 0, \end{array} \right. \end{aligned}$$

where the constraints are again imposed at the vertices of  $\mathcal{B}_p$ ,  $\Delta = \Delta_k \in \mathcal{V}(\mathcal{B}_p)$ . Using the optimizers,  $K_A$  and  $K_B$  are obtained as

$$K_A := Y_Z^{-1} V, \quad K_B := Y_Z^{-1} U. \quad (24)$$